Vol 15 No 8, August 2006
1009-1963/2006/15(08)/1855-09

Chinese Physics

© 2006 Chin. Phys. Soc.
and IOP Publishing Ltd

Simulating high Reynolds number flow in two-dimensional lid-driven cavity by multi-relaxation-time lattice Boltzmann method*

Chai Zhen-Hua(柴振华)[a], Shi Bao-Chang(施保昌)[a)b)†], and Zheng Lin(郑 林)[b]

[a] *State Key Laboratory of Coal Combustion, Huazhong University of Science and Technology, Wuhan* 430074, *China*

[b] *Department of Mathematics, Huazhong University of Science and Technology, Wuhan* 430074, *China*

(Received 24 December 2005; revised manuscript received 20 March 2006)

By coupling the non-equilibrium extrapolation scheme for boundary condition with the multi-relaxation-time lattice Boltzmann method, this paper finds that the stability of the multi-relaxation-time model can be improved greatly, especially on simulating high Reynolds number (Re) flow. As a discovery, the super-stability analysed by Lallemand and Luo is verified and the complex structure of the cavity flow is also exhibited in our numerical simulation when Re is high enough. To the best knowledge of the authors, the maximum of Re which has been investigated by direct numerical simulation is only around 50 000 in the literature; however, this paper can readily extend the maximum to 1000 000 with the above combination.

Keywords: multi-relaxation-time lattice Boltzmann method, non-equilibrium extrapolation scheme, high Reynolds number, lid-driven cavity flow

PACC: 4700, 0270, 0200

1. Introduction

As a mesoscopic numerical approach, the lattice Boltzmann method (LBM) is originated from the lattice-gas automaton (LGA),[1] but it overcomes some drawbacks of the LGA, such as large statistical noise, limited range of physical parameters, and non-Galilean invariance.[2] In the past few years, we have witnessed a rapid development of the method known as LBM, In comparison with the conventional numerical algorithms, the kinetic features of the LBM enable it to be more effective for simulating complex fluid flows, such as thermal flows,[3,4] multiphase flows,[5,6] porous media,[7,8] magnetohydrodynamic systems[9,10] and so on.

The multiple-relaxation-time (MRT) LBM, as the generalized LBM or the moment method, overcomes some obvious defects of the lattice Bhatnagar–Gross–Krook (LBGK) model, such as fixed Prandtl number and fixed ratio between the kinematic and bulk viscosities.[11,12] In addition, what should be mentioned is, compared with the popular LBGK model, which is also called the single-relaxation-time (SRT) LBM, the stability of the LBM can be improved greatly by incorporating the MRT scheme.[13] In recent years, the MRT LBM has attained more and more attention from many researchers, and been applied in many fields. However, to our knowledge, the striking stability was only analysed theoretically by Lallemand and Luo,[13] and it has not been validated in practical numerical simulation, especially when Re is high.

Numerical methods for two-dimensional steady incompressible Navier–Stokes equations are often tested on a very well known benchmark problem, the lid-driven cavity flow. Despite the fact that the geometry of the lid-driven cavity is very simple, the flow retains a rich fluid flow physics manifested by multiple counter-rotating recirculating regions on the corners of the cavity depending on the Reynolds number. In the literature, there are many numerical methods applied to this problem. The problem is studied extensively, but the investigated Re is finite. There is an interesting phenomenon, that many studies derive the same results only when $Re \leq 10000$, but there are few reports on higher Re, and this is an incentive to our study of this problem and attempt to give some illuminative results on high Re.

Among the numerous studies found in the liter-

*Project supported by the National Natural Science Foundation of China (Grant No 70271069).

†Corresponding author. E-mail:sbchust@yahoo.com

ature, it is necessary for us to give a brief survey of some of the significant studies on the lid-driven cavity flow. Ghia *et al* [14] have applied a multi-grid strategy and presented solutions for Reynolds numbers as high as $Re = 10000$ with a 257×257 lattice. Hou *et al* [15] have used LBM for simulating the cavity flow with a 256×256 lattice and presented solution up to Reynolds number of $Re = 7500$. Nallasamy and Prasad[16] have presented steady solutions for Reynolds number up to $Re \leq 50000$. Zhou *et al*[17] have investigated the solutions of driven cavity flow for Reynolds number as high as $Re = 52900$ with LBGK model. Ramšak and Škerget[18] have presented some steady solutions when Re up to 50000. Recently, Erturek *et al* [19] have pointed out that the solutions derived by Nallasamy and Prasad[16] is inaccurate due to excessive numerical dissipation caused by their first order upwind difference scheme and presented steady solutions for $Re \leq 21000$. In addition, it should be mentioned that the combination of LBM with subgrid model has been proposed by Hou[20] for simulating the two-dimensional lid-driven cavity flow up to a Reynolds number of 1000 000 on a 256×256 lattice.

The rest of this paper is organized as follows. In Section 2, the two-dimensional MRT LBM and the non-equilibrium extrapolation scheme for boundary treatment are introduced. In Section 3, numerical simulation on two-dimensional lid-driven cavity is performed for testing the super stability of the method and the Re is investigated to 1000 000. Summary and conclusions are given in Section 4.

2. The MRT LBM and the non-equilibrium extrapolation scheme

2.1. The MRT LBM

For the sake of simplicity without losing generality, we shall only consider the case of a simple nine-velocity on a square lattice, the nine possible velocities in the D2Q9 model are c_i, $i \in \{0, 1, 2, 3, 4, 5, 6, 7, 8\}$

$$c_i = \begin{cases} (0,0), & i = 0, \\ (\cos[(i-1)\pi/2], \sin[(i-1)\pi/2])c, & i = 1,2,3,4, \\ (\cos[(2i-9)\pi/4], \sin[(2i-9)\pi/4])\sqrt{2}c, & i = 5,6,7,8, \end{cases}$$

where $c{=}\Delta x/\Delta t$, Δx and Δt are the lattice grid space and time step respectively. In MRT LBM, c is usually set to be 1, i.e. $\Delta x = \Delta t$.

Recently, Lallemand and Luo[13] have concluded that MRT model could be used for improving the numerical stability of LBM, and performed the theoretical analysis on the dispersion, dissipation, isotropy, Galilean invariance, and stability characteristics of a generalized lattice Boltzmann equation model proposed by D'Humières.[11] In this paper, we will only pay attention to the MRT model, which is proposed by Lallemand and Luo.[13] In their model, a new column vector of macroscopic variables and the distribution functions are defined as follows:

$$|\varrho\rangle \equiv (\rho,\ e,\ \varepsilon,\ j_x,\ q_x,\ j_y,\ q_y,\ p_{xx},\ p_{xy})^{\top},$$

$$|f\rangle = (f_0(x,t),\ f_1(x,t),\ f_2(x,t),\ f_3(x,t),\ f_4(x,t),\ f_5(x,t),\ f_6(x,t),\ f_7(x,t),\ f_8(x,t))^{\top},$$

where $\top$ denotes the transpose operator, and $|\varrho\rangle$ is related to $|f\rangle$, the relation between them can be expressed as

$$|\varrho\rangle = M|f\rangle, \tag{1}$$

where

$$M = \begin{pmatrix} 1 & 1 & 1 & 1 & 1 & 1 & 1 & 1 & 1 \\ -4 & -1 & -1 & -1 & -1 & 2 & 2 & 2 & 2 \\ 4 & -2 & -2 & -2 & -2 & 1 & 1 & 1 & 1 \\ 0 & 1 & 0 & -1 & 0 & 1 & -1 & -1 & 1 \\ 0 & -2 & 0 & 2 & 0 & 1 & -1 & -1 & 1 \\ 0 & 0 & 1 & 0 & -1 & 1 & 1 & -1 & -1 \\ 0 & 0 & -2 & 0 & 2 & 1 & 1 & -1 & -1 \\ 0 & 1 & -1 & 1 & -1 & 0 & 0 & 0 & 0 \\ 0 & 0 & 0 & 0 & 0 & 1 & -1 & 1 & -1 \end{pmatrix},$$

which is a 9×9 matrix transforming $|f\rangle$ to $|\varrho\rangle$. In the column vector $|\varrho\rangle$, ρ is the density, e is the energy, ε is the square of the energy, j_x and j_y correspond to the x and y components of momentum, q_x and q_y correspond to the x and y components of energy flux, p_{xx} and p_{xy} correspond to the diagonal and off-diagonal component of the viscous stress tensor. One of the important advantages of the above MRT model is that macroscopic variables can be readily derived if the $|f\rangle$ is known. In addition, due to the conservation of the mass and momentum before and after collision, the total mass and momentum have no need to relax at all.

The evolution equation of the model is

$$|f_i(x + c_i\Delta t, t + \Delta t)\rangle - |f_i(x,t)\rangle = M^{-1}S[|\varrho(x,t)\rangle - |\varrho^{(\mathrm{eq})}\rangle], \tag{2}$$

where S is a diagonal relaxation matrix:

$$S = \mathrm{diag}(0, -s_2, -s_3, 0, -s_5, 0, -s_7, -s_8, -s_9), \tag{3}$$

$|\varrho^{(\mathrm{eq})}\rangle$ is the equilibrium values of the $|\varrho(x,t)\rangle$, which can be written as[13]

$$|\varrho^{(\mathrm{eq})}\rangle = (\rho,\ e^{(\mathrm{eq})},\ \varepsilon^{(\mathrm{eq})},\ j_x,\ q_x^{(\mathrm{eq})},\ j_y,\ q_y^{(\mathrm{eq})},\ p_{xx}^{(\mathrm{eq})},\ p_{xy}^{(\mathrm{eq})})^{\top}, \tag{4}$$

where the equilibrium values of the non-conserved moments in the above equations $e^{(\mathrm{eq})}, \varepsilon^{(\mathrm{eq})}, q_x^{(\mathrm{eq})}, q_y^{(\mathrm{eq})}, p_{xx}^{(\mathrm{eq})}$ and $p_{xy}^{(\mathrm{eq})}$ can be also derived from the following equations:[13]

$$\begin{aligned} e^{(\mathrm{eq})} &= -2\rho + 3(j_x^2 + j_y^2), \\ \varepsilon^{(\mathrm{eq})} &= \rho - 3(j_x^2 + j_y^2), \\ q_x^{(\mathrm{eq})} &= -j_x, \\ q_y^{(\mathrm{eq})} &= -j_y, \\ p_{xx}^{(\mathrm{eq})} &= j_x^2 - j_y^2, \\ p_{xy}^{(\mathrm{eq})} &= j_x \times j_y. \end{aligned} \tag{5}$$

It should be mentioned that the evolution process of the MRT model still consists of two parts: collision and propagation. The collision is executed in momentum space

$$|f_i^{+}(x,t)\rangle = |f_i(x,t)\rangle + M^{-1}S[|\varrho(x,t)\rangle - |\varrho^{(\mathrm{eq})}\rangle], \tag{6}$$

but the propagation is executed in velocity space

$$|f_i(x + c_i\Delta t, t + \Delta t)\rangle = |f_i^{+}(x,t)\rangle. \tag{7}$$

Therefore, the evolution process includes the transformation between the momentum space and the velocity space.

In addition, in order to let the density do not appear in the terms j_x and j_y, we also choose a modified equilibrium distribution function proposed by He and Luo,[21]

$$f_i^{(\mathrm{eq})} = w_i\left\{\rho + \rho_0[3(c_i \cdot u) + \frac{9}{2}(c_i \cdot u)^2 - \frac{3}{2}u^2]\right\},$$

where w_i is weight coefficients of the equilibrium distribution function, $w_0 = 4/9, w_1 = w_2 = w_3 = w_4 = 1/9, w_5 = w_6 = w_7 = w_8 = 1/36$, the mean density ρ_0 is usually set to be 1.0 in numerical simulation.

2.2. The non-equilibrium extrapolation scheme

As Chen[22] said, 'To a certain degree, achieving self-consistent boundary conditions with a given accuracy is as important as developing numerical schemes themselves', which expresses that the treatment for boundary condition is so crucial in LBM. MRT model is more stable than the LBGK model, but the influence of treatment for the boundary condition is not considered by Lallemand and Luo.[13] D'Humières *et al*[12] also have pointed out that the local analysis of

MRT model does not consider boundary conditions and therefore the system may be less stable in actual simulations. So finding a scheme for the boundary condition which is compatible with the MRT model is also important in simulating complex fluid flows. Until now, many investigations have been carried out and several schemes have been proposed, such as bounce back scheme, kinetic scheme, specular reflection scheme, etc. Recently, the non-equilibrium extrapolation scheme is proposed by Guo *et al*[23] for the boundary condition, which is a second-order scheme in numerical accuracy and compatible with the accuracy of the LBM. Through mass numerical experiments and comparison with other schemes, we find that the globe stability of the MRT can be further improved by coupling the non-equilibrium extrapolation scheme. The superiority of the MRT model is exhibited in our numerical experiments.

The boundary condition is usually given by macroscopical variables, such as velocity or pressure. The distribution function $f_i(x,t)$ is usually not given directly at the boundaries. Therefore, we must determine the distribution function at the boundaries from the given macroscopic variables. Suppose $x_{\rm b}$ lies at the boundary and $x_{\rm f}$ is the nearest node in the fluid, and notice that the distribution function $f_i(x_{\rm b},t)$ can be decomposed into its equilibrium and non-equilibrium parts,

$$f_i(x_{\rm b},t) = f_i^{(\rm eq)}(x_{\rm b},t) + f_i^{(\rm neq)}(x_{\rm b},t), \qquad (8)$$

where $f_i^{(\rm eq)}(x_{\rm b},t)$ and $f_i^{(\rm neq)}(x_{\rm b},t)$ are equilibrium and non-equilibrium parts of $f_i(x_{\rm b},t)$ respectively. Generally speaking, between the two macroscopic variables in $f_i^{(\rm eq)}(x_{\rm b},t)$, density ρ and velocity u, only one is given by the boundary condition. In the non-equilibrium extrapolation scheme, the unknown macroscopic variable is replaced by the known macroscopic variable at the node $x_{\rm f}$, and $f_i^{(\rm neq)}(x_{\rm b},t)$ in Eq.(8) can be replaced by $f_i^{(\rm neq)}(x_{\rm f},t)$, so we can derive all the unknown distribution functions at the boundary from Eq.(8).

3. Numerical experiments

Numerical experiments are implemented on a two-dimensional lid-driven cavity and the investigated Re ranges from 20 000 to 1000 000. The two-dimensional lid-driven cavity has been investigated by many researchers with several kinds of methods.[15,17,19,24] However, the maximum of Reynolds number in their simulations is only around 50 000 and the presented results have not apparent differences. Compared with these existing results, the aim of the present work is to verify the striking stability of MRT model, and simultaneously the shape and structure of the flow in the lid-driven cavity are investigated when Re is very high.

3.1. Selection of relaxation parameter

The configuration of the lid-driven cavity considered in this paper consists of a two-dimensional square cavity whose top plate moves from left to right with a uniform velocity U_0, while the other three walls are fixed. In our simulation, U_0 is set to be 0.1, the Reynolds number is defined in the problem as

$$Re = LU_0/\nu, \qquad (9)$$

where $L = 1$ is the height and width of the cavity, ν is the kinematic viscosity which is defined as

$$\nu = \frac{1}{3}(\tau - \frac{1}{2})\Delta t, \qquad (10)$$

so the relaxation time can be obtained from the Eqs.(9) and (10) as

$$\tau = 3U_0/(\Delta t\, Re) + 1/2, \qquad (11)$$

the relaxation parameters in Eq.(11) can be chosen as s_1=s_4=s_6=0, s_2=1.1, s_3=1.0,s_5=s_7=1.2, s_8=s_9=$\dfrac{1}{\tau}$.

3.2. Numerical results

Before demonstrating the results on high Re, the accuracy of the MRT model is first tested through the numerical comparison with other models, and the detailed results listed in Table 1.

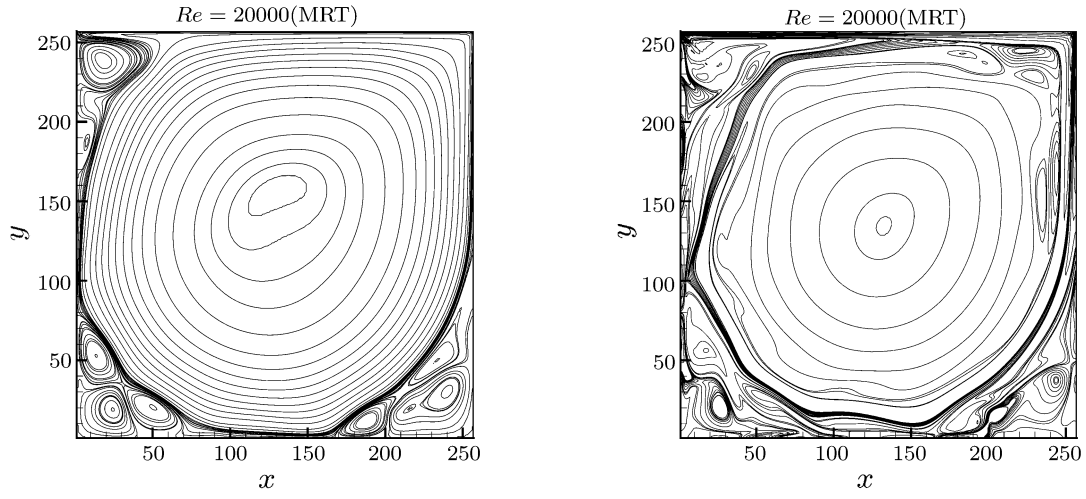
Subsequently, numerical simulations are carried out on a 257×257 lattice for Re from 20 000 to 100 000, 513×513 lattice for Re=500 000 and Re=1000 000; the corresponding relaxation parameter $w = 1/\tau$ can be derived from Eq.(11) as 1.984 757 (Re=20 000), 1.993 875 (Re=50 000), 1.996 933 (Re=100 000), 1.998 772 (Re=500 000) and 1.999 386 (Re=1000 000). To make the behaviour of the flow numerically stable, the iterative time step must be long enough, which is fixed at 1000 000 in all numerical experiments. Here, some results including the streamlines, the velocity, the mean velocity and the root-mean-square (rms) velocity along vertical and horizonal lines at various Reynolds number are presented in the following figures.

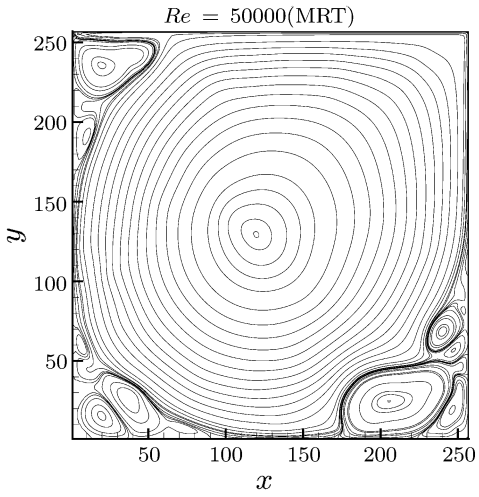
Table 1. The locations (x, y) of primary and secondary vortices

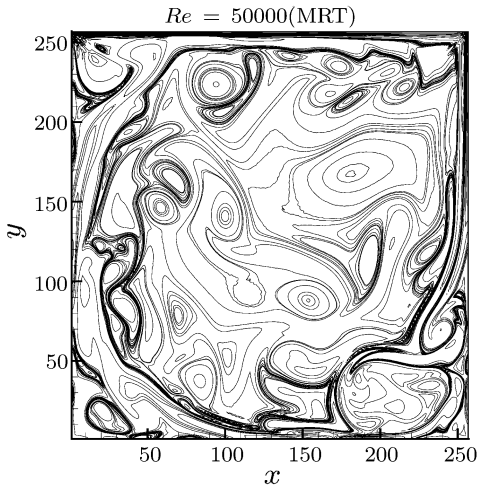
Re	model	x_c	y_c	x_l	y_l	x_r	y_r
5000	MRT	0.5156	0.5352	0.0742	0.1328	0.8086	0.0742
	SRT	0.5195	0.5352	0.0742	0.1328	0.8086	0.0742
	Ghia.U	0.5117	0.5352	0.0703	0.1367	0.8086	0.0742
	Hou	0.5176	0.5373	0.0784	0.1373	0.8078	0.0745
	Erturk.E	0.5150	0.5350	0.0733	0.1367	0.8050	0.0733
7500	MRT	0.5117	0.5352	0.0664	0.1486	0.7891	0.0664
	SRT	0.5156	0.5352	0.0742	0.1328	0.8047	0.0742
	Ghia.U	0.5117	0.5322	0.0645	0.1504	0.7813	0.0625
	Hou	0.5176	0.5333	0.0706	0.1529	0.7922	0.0667
	Erturk.E	0.5133	0.5317	0.0650	0.1517	0.7900	0.0650
10000	MRT	0.5117	0.5313	0.0469	0.1593	0.7773	0.0586
	SRT	0.5117	0.5313	0.0625	0.1563	0.7813	0.0625
	Erturk.E	0.5117	0.5300	0.0583	0.1633	0.7767	0.0600
20000	MRT	0.5078	0.6094	-	-	-	-
	SRT	0.4883	0.5703	-	-	-	-
	Erturk.E	0.5100	0.5267	-	-	-	-

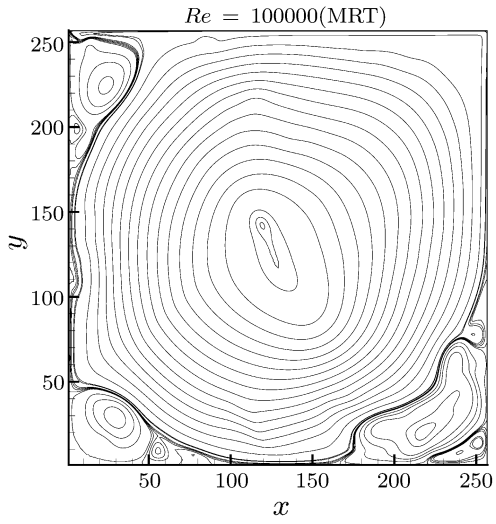
(x_c, y_c): the location of primary vortex, $(x_{l,r}, y_{l,r})$: the locations of secondary vortex in the bottom corners.

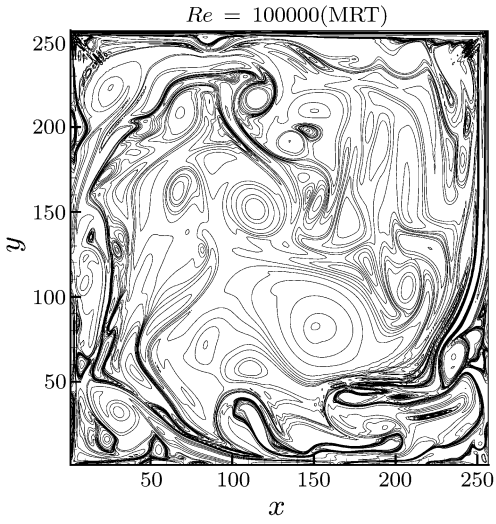
From Fig.1, we can derive that the flow region near the wall is the first part changed into turbulence, but different parts of the flow domain remain at different levels of turbulence activity and some parts may remain laminar even though unsteady when Re is up to 20 000. However, when $Re \geq$50 000, the flow in the cavity becomes turbulent completely, even though the plot of streamline for Re =50 000 shows a relatively stable primary vortex, however, the shape and the structure of flow change greatly with time, this can be validated by the plot of vortex. When Re is increased to 100 000, the core of primary vortex changes apparently and rotates with time, and the secondary vortices become more oscillating. For Re as high as 500 000, there is no apparent or strict primary vortex in the middle domain. When Re is further increased to 1000 000, many small vortices appear in the middle domain of the cavity, the whole domain becomes more unordered than that reported in Ref.[20]. Apart from looking at the distribution of components of the velocity and the mean velocity on the centrelines at various Re in Figs.2 and 3, it will be quite instructive to see how the rms velocity is distributed. The profiles of the rms velocity on different centrelines at various Re are presented in Fig.4. These plots show clearly the effects of the high Re on the related pattern and some results agree well with those reported by Hou.[20]

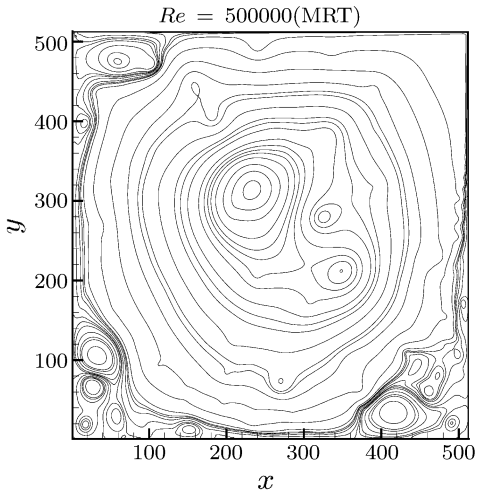


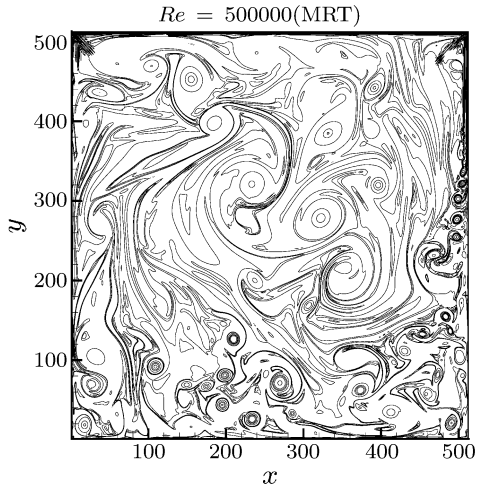

Re = 50000(MRT)
250
200
150
100
50
y
50 100 150 200 250
x


Re = 50000(MRT)
250
200
150
100
50
y
50 100 150 200 250
x


Re = 100000(MRT)
250
200
150
100
50
y
50 100 150 200 250
x


Re = 100000(MRT)
250
200
150
100
50
y
50 100 150 200 250
x


Re = 500000(MRT)
500
400
300
200
100
y
100 200 300 400 500
x


Re = 500000(MRT)
500
400
300
200
100
y
100 200 300 400 500
x

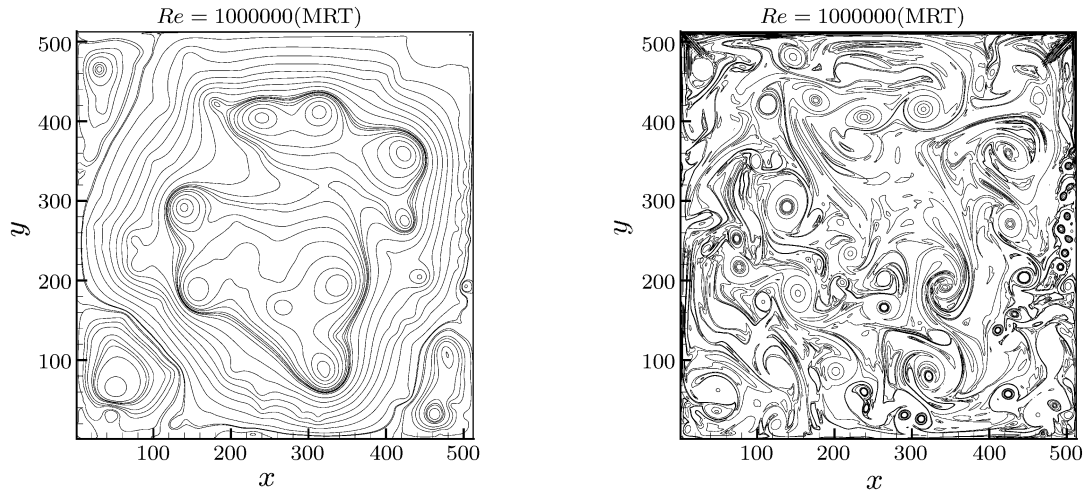


Fig.1. The streamline and vortex contours of Re=20000, 50000, 100000, 500000, 1000000.

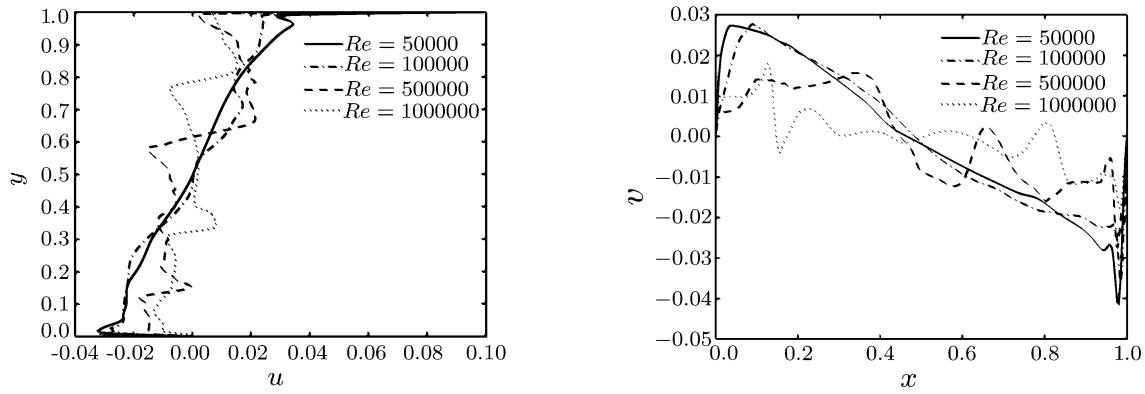


Fig.2. Computed u-velocity and v-velocity profiles on different centrelines at various Reynolds numbers.

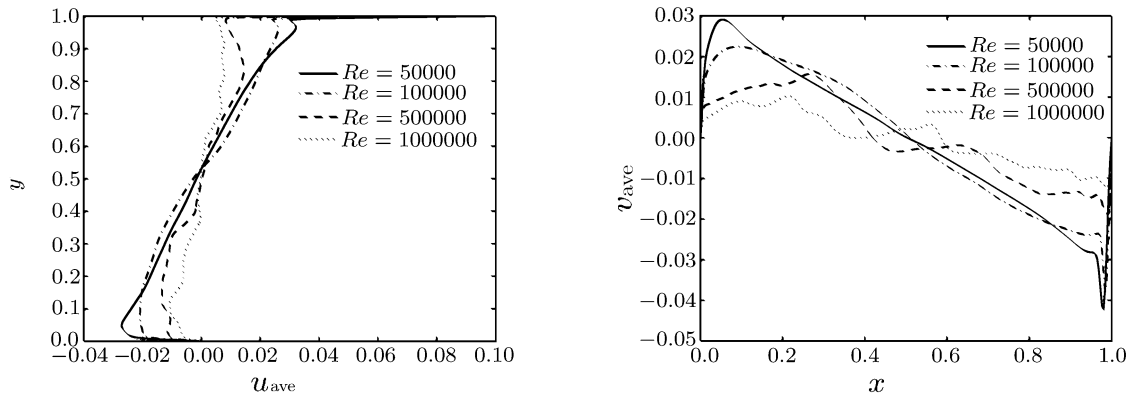


Fig.3. The time-averaged velocity profiles on different centrelines at various Reynolds numbers.

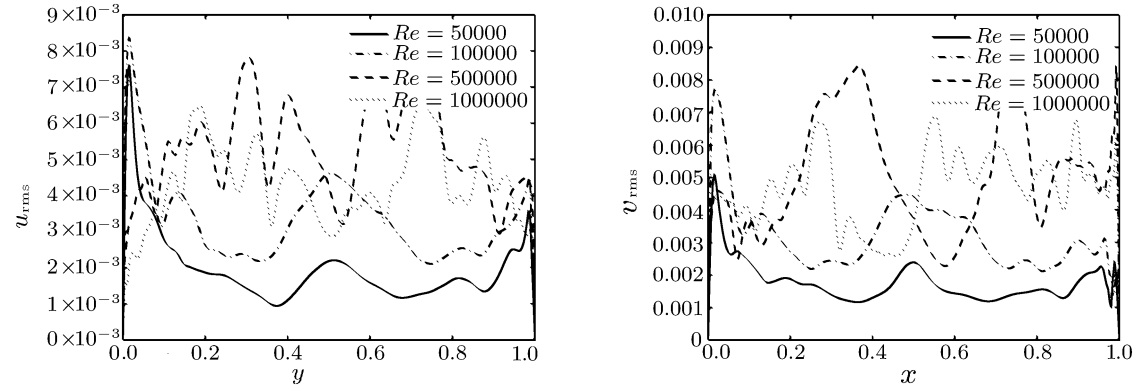


Fig.4. The root-mean-square (rms) velocity profiles of u and v on different centrelines at various Reynolds numbers.

With the increase of the Re, especially when the flow changed into turbulence, the requirement for precision becomes more important and must be considered in practical numerical experiments. To present an accurate result, the grid must be fine enough; however, due to the constraint of the computer's efficiency, the finest grid in the present work is only 1025×1025. As an example, the effect of the grid is taken account of only for Re=1000 000; we find that the effect of grid on the time-averaged velocity profiles on different centrelines is very important. There is an important changing point when the lattice is in the transition from 257×257 to 513×513; however, there is no great change when much finer lattice 1025×1025 is applied, so the 513×513 lattice may be enough for forecasting the time-averaged structures of the flow. We also find that the plots of the time-averaged velocity profiles on centrelines are closer to the low Re case (Fig.3) with the finer grid, which can be a reason for us to conclude that the results derived may be wrong when the coarse grid is applied; the detailed results are presented in Fig.5.

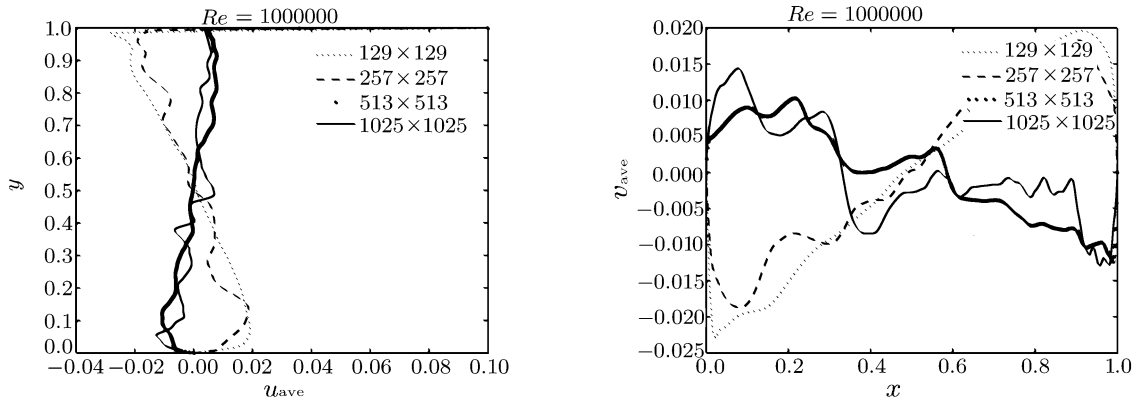


Fig.5. The time-averaged velocity profiles on different centrelines at different sizes of lattice.

It is a pity that there is no detailed literature on simulating high Re flow in two-dimensional lid-driven cavity, and no numerical results or experimental data for verifying our numerical experiment. Further study is needed.

4. Summary and conclusion

In the current study, the striking stability of MRT model is further verified in our numerical simulation, and some preliminary results for high Re flow in two-dimensional cavity are presented. As for accuracy, further study is greatly needed. The research work of this paper can be seen as a continuation of our previous work;[17,25,26] it is a little premature for us to conclude that the MRT model can provide an exact solution for lid-driven cavity flow due to lack of comprehensive comparable results from direct numerical simulation and experimental investigation under high Re condition. However, it opens a door for us to understand the behaviour of flow when Re is high enough. In addition, it should be mentioned that the non-equilibrium extrapolation scheme for boundary condition also plays an important role in our simulation, when other popular scheme for boundary, such as the bounce back scheme, is coupled with MRT model, the maximum of Re which can be tested is only about 10000. In fact, much higher Re also can be tested by the proposed combination in this paper as long as relaxation parameter $w < 2$(stable condition). In future, the accuracy for presented results needs to be verified by parallel computation with much finer grid.

Acknowledgments

Authors would like to thank Dr Guo Zhao-Li, Dr McCracken M, Dr Du Rui and Chen Xing-Wang for useful discussions.

References

[1] Frisch U, Hasslacher B and Pomeau Y 1986 *Phys. Rev. Lett.* **56** 1505

[2] Higuera F, Succi S and Benzi R 1989 *Europhys. Lett.* **9** 663

[3] He X Y, Chen S Y and Doolen G D 1998 *J. Comput. Phys.* **146** 282

[4] Shi Y, Zhao T S and Guo Z L 2004 *Phys. Rev.* E. **70** 066310

[5] Shan X W and Chen H D 1993 *Phys. Rev.* E. **47** 1815
[6] Guo Z L and Zhao T S 2003 *Phys. Rev.* E. **68** 035302
[7] Xu Y S, Zhong Y J and Huang G X 2004 *Chin. Phys. Lett.* **21** 2454
[8] Guo Z L and Zhao T S 2002 *Phys. Rev.* E. **66** 036304
[9] Dellar P 2002 *J. Comput. Phys.* **179** 95
[10] Chen X W and Shi B C 2005 *Chin. Phys.* **14** 1398
[11] D'Humières 1992 in *Rarefied Gas Dynamics: Theory and Simulations, Progress in Astronautics and Aeronautics* edited by Shizgal B D and Weaver P D (AIAA Press, Washington, DC) **159** 450
[12] D'Humières, Ginzburg I, Krafczyk M, Lallemand P, Luo L S *et al* 2002 *Phil. Trans. R. Soc. Lond.* A **360** 437
[13] Lallemand P and Luo L S 2000 *Phys. Rev.* E. **61** 6546
[14] Ghia U, Guia K N and Shin C T 1982 *J. Comput. Phys.* **48** 387
[15] Hou S L, Chen S Y, Zou Q S, Doolen G D and Cogley A C 1995 *J. Comput. Phys.* **118** 329
[16] Nallasamy M and Prasad K 1977 *J. Fluid. Mech.* **79** 391
[17] Zhou X Y, Shi B C and Wang N C 2004 *Chin. Phys.* **13** 712
[18] Ramšak M and Škerget L 2004 *Int. J. Numer. Meth. Fluids.* **46** 815
[19] Erturek E, Corke T C and Gökçöl C 2005 *Int. J. Numer. Meth. Fluids.* **48** 747
[20] Hou S L 1995 *Ph.D thesis* (Kansas State University. Manhattan, Kansas)
[21] He X Y and Luo L S 1997 *J. Stat. Phys.* **88** 927
[22] Chen S Y and Martinez D 1996 *Phys. Fluids* **8** 2527
[23] Guo Z L, Zheng C G and Shi B C 2002 *Chin. Phys.* **11** 366
[24] Barragy E and Carey G F 1997 *Comput. Fluids* **26** 453
[25] Shi B C, Wang N C, Guo W B and Guo Z L 2001 *Proc. of DCABES*2001 (Wuhan: Hubei Sci. & Tech. Press) 108-112
[26] Guo W B, Shi B C, Wang N C and Guo Z L 2002 *Computer. Appl.* **22** 1 (in Chinese)